Enantiomeric Separation of Racemic Neolignans on Chiralcel OD and Determination of Their Absolute Configuration with Online Circular Dichroism

Krisztina Kónya[1], Attila Kiss-Szikszai[2], Tibor Kurtán[1], and **Sándor Antus[1,*]**

[1]Department of Organic Chemistry, University of Debrecen, P.O. Box 20 and [2]Research Group for Carbohydrates of the Hungarian Academy of Sciences, P.O. Box 55, H-4010 Debrecen, Hungary

Abstract

Effective enantiomeric separations of erythro- and threo-8.O.4'-neolignans with different aromatic substitution pattern (1a-i, 2a-i) are achieved on the commercially available chiral stationary phase cellulose tris(3,5-dimethylphenylcarbamate) (Chiralcel OD). It is shown that the chiral recognition of the stationary phase is significantly dependent on the substitution pattern of the racemic compounds. Online liquid chromatography (LC)–circular dichroism (CD) analysis allows for the establishment of a correlation between the absolute configuration of the separated erythro-8.O.4'-neolignans and their characteristic CD transitions, which could be used to determine or revise the configuration of previously isolated erythro-8.O.4'-neolignans. Although the absolute configurations of threo-isomers is not determined unambiguously from the LC–CD analysis, it is proven that both their elution order and chiroptical properties are significantly influenced by the substitution pattern of the aromatic rings.

Introduction

The 8.O.4'-type neolignans represent a small subgroup of naturally occurring phenylpropanoid dimers whose members have been isolated from the plants of nutmeg (*Myristica fragrans Houtt.*) (1–5), ucuba oiltree (*Virola surinamensis*) (6), *Virola caritane* (7), and epena (*Virola pavonis*) (8). Recently, an efficient approach for the synthesis of racemic erythro- and threo-8.O.4'-neolignans (**1a-i**, **2a-i,** respectively, Figure 1) has been published (9), and the threo-series (**2a-i**) has been shown to possess significantly higher activity in the inhibition of the oxidative burst of human polymorphonuclear leukocytes (PMNLs) than their erythro stereoisomers (**1a-i**) (10). The erythro and threo relative configurations of these stereoisomers were assigned on the basis of their coupling constants $J_{H\text{-}7,H\text{-}8}$, which were found to be 3 Hz for the erythro and 6–8 Hz for the threo compounds (9).

In order to gain further insights into the structural requirements of the antioxidant activity of these natural products, we set our sights on their enantiomeric separation by high-performance liquid chromatography (HPLC) using cellulose tris(3,5-dimethylphenylcarbamate) (CTPC) (Chiralcel OD) as the chiral stationary phase (CSP). The published characteristics of this CSP (11–14) suggested that, because of their hydroxy group at C-7 and the etheric oxygen at C-8, this type of neolignans may form a strong interaction with the polar carbamate groups of the CSP via hydrogen bonding. Moreover, a π–π interaction between the aryl groups of the CSP and the aromatic moieties of the neolignans **1a-i** and **2a-i** could also be predicted. Once the enantiomers are separated, their online liquid chromatography (LC) and circular dichroism (CD) analysis can be used for their optical charactization and potential configurational assignment, and it can also

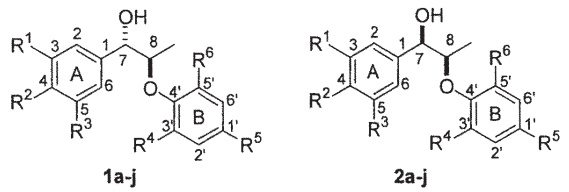

1, 2	R^1	R^2	R^3	R^4	R^5	R^6
a	OMe	OMe	H	OMe	allyl	OMe
b	OMe	OMe	OMe	OMe	allyl	OMe
c	O-CH_2-O		H	OMe	allyl	OMe
d	OMe	OMe	H	H	allyl	OMe
e	OMe	OMe	OMe	H	allyl	OMe
f	O-CH_2-O		H	H	allyl	OMe
g	OMe	OMe	H	H	(E)-propenyl	OMe
h	OMe	OMe	OMe	H	(E)-propenyl	OMe
i	O-CH_2-O		H	H	(E)-propenyl	OMe
j	H	H	H	H	H	H

Figure 1. Structures of erythro-(**1a-i**) and threo-8.O.4'-neolignans (**2a-i**), **1j**, and **2j**. The compound numbers **1a** through **1j** represent structures with erythro configuration and with different substitution patterns, and compounds **2a** through **2j** have threo configurations.

* Author to whom correspondence should be addressed: email antuss@tigris.klte.hu.

report whether the aromatic substituents have an effect on the elution order and the CD properties.

Experimental

Instrumentation

Chromatography was performed on the Chiralcel OD column (250 × 4.6 mm, 10 µm) (Daicel Chemical Industries, Osaka, Japan) with a JASCO-type HPLC system that included a PU-980 HPLC pump and MD-910 multiwavelength detector (JASCO, Easton, MD). The LC–CD and LC–UV chromatograms were recorded online on a JASCO J-810 spectropolarimeter equipped with an HPLC flow cell. The online UV and CD spectra were consequently recorded at the maxima of the CD peaks where the flow was stopped.

Materials

HPLC-grade *n*-hexane and 2-propanol were purchased from Merck (Darmstadt, Germany) (LiChrosolv quality for LC). Racemic erythro- and threo-8.O.4'-neolignans, **1a-i** and **2a-i,** respectively, were prepared by known methods (9,10) from 2-phenoxypropiophenon under the conditions described in the literature (9).

Chromatographic conditions

The mobile phase consisted of HPLC-grade *n*-hexane and 2-propanol (90:10), which were premixed before use. The flow rate of the mobile phase was 0.9 mL/min except for the cases of **1j** and **2j** (0.5 mL/min), and the column was operated at room temperature (~ 24°C). UV detection was performed at 280 nm. The retention factor (k') was determined by:

$$k' = (t_R - t_0)/t \qquad \text{Eq. 1}$$

The retention time (t_0) was taken as the time when the eluent was injected.

Result and Discussion

HPLC analysis

Chromatographic data for the enantiomers of erythro- and threo-8.O.4'-neolignans (**1a-i** and **2a-i**, respectively) and related compounds (**1j**, **2j**, **1k**, and **2k**) separated on CTPC (given in Table I) at room temperature with a mobile phase of *n*-hexane–2-propanol (90:10) at a flow rate of 0.9 mL/min [except for the cases of **1j**, **2j**, **1k**, and **2k** (0.5 mL/min)]. Under these conditions, most of the racemates gave baseline resolution, and their characteristic chromatographic profiles are shown in Figure 2. It was only **1e** from the erythro-derivatives (**1a-i**) and **2a** and **2f** from the threo-compounds (**2a-i**) that could not be separated on this CSP. The comparison of the chromatographic data of the erythro-derivatives (**1a-i**) with those of the corresponding threo-derivatives (**2a-i**) has indicated that apparently the relative configuration of the solute (7*S*,8*R* or 7*S*,8*S*; 7*R*,8*S* or 7*S*,8*R*) does not play a decisive role in the chiral recognition of the CSP. This fact was also supported by the successful resolution of the unsubstituted compounds (**1j,2j**), whose stereoisomers could be baseline separated (**1j**: R_s = 1.42; **2j**: R_s = 1.82).

Okamoto et al. (11,12,15) have already clearly shown the successful resolution of solutes that are able to interact with the NH and C=O groups of CSP by hydrogen bonding. Moreover, dipole–dipole and π–π interactions can also be predicted on CTPC. In order to check the role of the 7-OH of **1j** and **2j** in the

Table I. HPLC Parameters of Erythro-(1a-i) and Threo-8.O.4'-Neolignans (2a-i), 1j, k, and 2j, and k

Compound	$t_{R(1)}$	k'$_1$	$t_{R(2)}$	k'$_2$	α	R_s
1a	20.81	3.94	21.77	4.17	1.06	0.91
2a	29.84	6.08	–		–	
–	–					
1b	17.38	3.13	18.43	3.37	1.08	0.95
2b	22.49	4.34	32.93	6.82	1.57	5.32
1c	10.08	1.39	13.29	2.16	1.55	5.33
2c	14.40	2.42	17.39	3.13	1.29	3.49
1d	20.81	3.94	26.84	5.37	1.36	4.18
2d	24.84	4.90	37.92	8.00	1.63	6.28
1e	17.97	3.27	–	–	–	–
2e	19.75	3.69	25.76	5.11	1.39	3.43
1f	10.97	1.60	12.89	2.06	1.28	3.24
2f	14.68	2.48	–	–	–	–
1g	23.60	4.60	31.76	6.54	1.42	4.71
2g	27.31	5.48	36.25	7.6	1.39	3.67
1h	21.65	4.14	28.48	5.76	1.39	3.98
2h	23.11	4.48	30.25	6.18	1.38	4.00
1i	12.68	2.01	17.60	3.18	1.58	6.17
2i	15.35	2.64	16.15	2.83	1.07	1.07
1j	19.75	3.11	20.93	3.36	1.03	1.42
2j	19.79	3.12	21.52	3.48	1.12	1.84
1k (1jAc)a	11.47	1.39	12.77	1.66	1.20	1.02
2k (2jAc)a	12.13	1.53	–	–		–
–						

* The flow was 0.9 mL/min in all measurement, and all of the chromatograms were

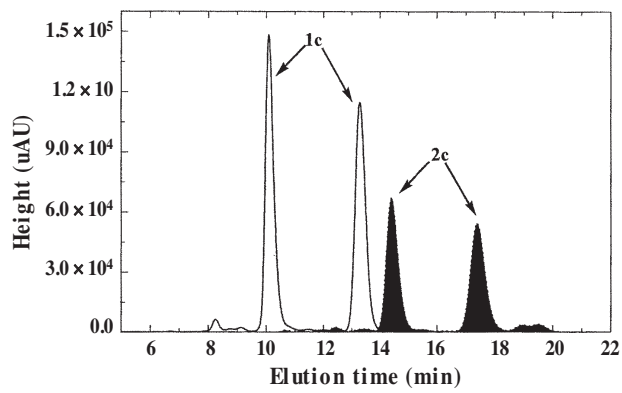

Figure 2. Juxtaposed HPLC chromatogram of the **1c** erythro- and the **2c** threo-isomers with baseline separation of the enantiomers.

chiral recognition process, their acetyl derivatives **1k** and **2k,** respectively, were also studied. Interestingly, the chiral recognition of CTPC is lost in the case of the threo-derivative **2k**, but in the case of **1j** the introduction of the acetyl group (**1j**→**1k**) has significantly smaller influence on the chiral discrimination (**1j**: R_s = 1.42; **1k**: R_s = 1.02).

On the basis of this result, it could be concluded that not only the hydrogen bonding between the CPS and solute but also the dipole–dipole or π–π interactions seem to be important for an efficient chiral discrimination. The comparison of the separation data of **1f** and **2f** (R_s, α) with those of **1i** and **2i**, respectively, has suggested that, besides the polar interactions, the π–π interaction between their aryl moieties and the aromatic groups of the CTPC situated outside of the helical cellulose backbone (16) may be involved strongly in the chiral discrimination of the CTPC. Thus, the presence of a conjugated propenyl side chain of *trans* (E)-geometry in **1i** and **2i** increased the π-character of the molecule and, therefore, its interaction with the CPS, which resulted in an enhanced separation (**1f**, **1i**: R_s = 3.24, 6.17 resp.: **2f**, **2i**: R_s = 0.00, 1.07 resp.) both in the erythro- and the threo-isomers of compound **i**. It is also remarkable that this influence was found to be much more significant at the erythro configuration.

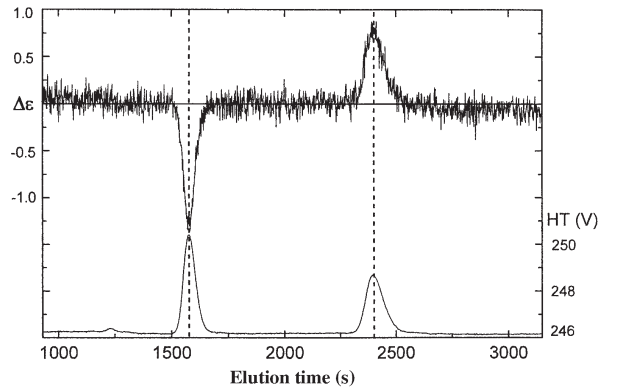

Figure 3. Online LC–CD and LC–UV chromatogram of the enantiomers of **2d** monitored at 230 nm.

Table II. CD Data of Erythro-8.O.4'-Neolignans (1a-d and 1f-h) Obtained by LC–CD Measurement

Compound	CD data in hexane–isopropanol 9:1 [nm (Δε)]		
1a	280 (–1.08)sh, 275 (–1.13), 265 (–0.88)	244 (–10.43)	229 (1.95)
1b	278 (–1.27), 270 (–1.30)	243 (–10.58)	230 (2.21)
1c	296 (–0.59)sh, 290 (–0.87)sh, 281 (–1.35)	246 (–8.35)	217 (–1.55)
1d	278 (–1.78)	239 (–9.52)	226 (0.39), 216 (–1.63)sh, 209 (–7.19)
1f	294 (–0.60)sh, 283 (–1.71)	239 (–6.79)	224 (–1.95)sh
1g	310 (–1.07)sh, 299 (2.15)sh, 289 (–2.38)	255 (–6.03)	234 (6.20)
1h	312 (–0.67)sh, 294 (–1.78), 277 (–1.93)sh,	263 (5.00)sh 256 (–6.35)	235 (5.21)

LC–CD analysis

The separation of the enantiomers of the erythro- (**1a-h**) and threo-derivatives (**2a-h**), except for those of **2a**, **1e**, and **2f**, were also followed by online CD detection and monitoring at a suitable wavelength between 230 and 245 nm with an LC–CD flow cell (see the LC–CD chromatogram of **2d** in Figure 3 and the Experimental section). The flow was stopped at the maxima of the CD signals, and the CD specra were recorded in the range of 200–350 nm. Because the UV spectra were recorded in parallel with the CD spectra, the measured absorbance could be used to determine the actual concentration in the flow cell provided that the extinction coefficients (ε) were known from the UV measurement of the racemic compounds with a known concentration. The LC–CD spectra could be recorded successfully even in cases (**1a** and **1b**) in which the resolution factor (R_s) was less than 1.0, and thus the peaks of the two enantiomers were partially overlapped.

The measured CD data (Table II) allowed for the configurational assignment of the separated erythro-enantiomers (**1a-h**) on the basis of Arnoldi and Merlini's CD results (17). They observed positive Cotton effects in the range of 230–290 nm with maxima at 268 and 230 nm (Δε = 0.86 and 4.76 in $CHCl_3$, respectively) for the 7*R*,8*S* configuration of the erythro-derivative **3** (Figure 4) obtained by asymmetric synthesis (17). Because the additional two methoxy groups of the ring A and the allyl group of ring B are not expected to change the characteristic CD bands of the erythro-derivative **1d**, compared with **3**, the negative maxima of its first eluted enantiomer at 278 and 239 nm (Δε = –1.78 and –9.52, respectively) derive from the 7*S*,8*R* absolute configuration (Figure 5). In the erythro-derivatives **1a**, **1b**, **1c**, and **1f**, the different substitution pattern caused only some wavelength shift in the range of 230–300 nm, although the sign of the characteristic CD bands remained the same (Table II). Thus, the 7*S*,8*R* absolute configuration could be unambiguously assigned to the first eluted peaks of these compounds as well. It is noteworthy that the sign of their CD bands below 230 nm were sensitive to the substitution pattern and, therefore, this region was not suitable for a safe configurational assignment. Compounds **1g** and **1h** contained a conjugating *trans*-propenyl side chain on the ring B, which red-shifts the CD transitions; namely, the intense 239 nm transition of **1d** appeared at 255 nm in **1g** (Figure 6 and Table II). The CD spectra of the first eluted peaks of **1g** and **1h** were practically the same, and their low-energy CD transitions between 245 and 320 nm were negative, which determined the 7*S*,8*R* configuration of the first eluted peaks.

CD spectroscopy has been widely used as a single tool for the configurational assignment of erythro-8.O.4'-neolignans (18,19), although the argument of the assignment is not always straightforward. For instance, Matsuda et al. (18)

used chiroptical data to determine the absolute configurations of two isolated erythro-8.O.4'-neolignans **4** and **5** (Figure 4) as 7*S*,8*R*. On the basis of the Nuclear Overhauser Effect experiments, they suggested that there is an exciton coupled interaction between the two aryl moieties that can be used for the assignment, although only one CD band around 239 nm (**4**: Δε = 1.94; **5**: Δε = 1.76) is reported in the experimental section instead of the expected two (18). The neolignans **4** and **5** are close structural analogues of **1d**, whose CD spectrum (Figure 5), however, shows no sign of exciton coupled interaction. Our LC–CD results prove that the intense negative CD bands around 240 nm (and the negative ones around 280 nm) derive from 7*S*,8*R* absolute configuration of erythro-8.O.4'-neolignans, which implies that the reported configurations of compounds **4** and **5** have to be changed to 7*R*,8*S*. This correlation between the CD properties and absolute configuration allows the configurational assignments of isolated erythro-8.O.4'-neolignan derivatives whose CD spectra were reported but the configuration could not be determined (20,21).

Greca et al. (19) used the CD results of Arnoldi and Merlini (17) to deduce the configuration of the erythro-8.O.4'-neolignan glucoside **6** and the erythro-8.O.3'-neolignan glucoside **7** (Figure 4) containing *trans*-propenyl side-chain on ring B. As we have shown, the conjugating *trans*-propenyl side-chain red-shifts the characteristic CD maximum of Arnoldi and Merlini from 230 nm to 255 and 256 nm in **1g** and **1h**, respectively (Figure 6 and Table II). Furthermore, the CD spectra of both **1g** and **1h** showed an oppositely signed maximum at around 235 nm compared with the sign of the characteristic 255 and 256 nm maxima. It is very likely that Greco et al. (19) mistakenly treated the negative CD bands of **6** and **7** at 230 and 228 nm (Figure 4) as the corresponding transition of Arnoldi and Merlini's characteristic CD bands at 230 nm and did not even report the positive CD data above 254 nm. If the assignments of those CD bands were indeed false and the low-energy transitions are positive, the configurational assignments of **6** and **7** would have to be inversed.

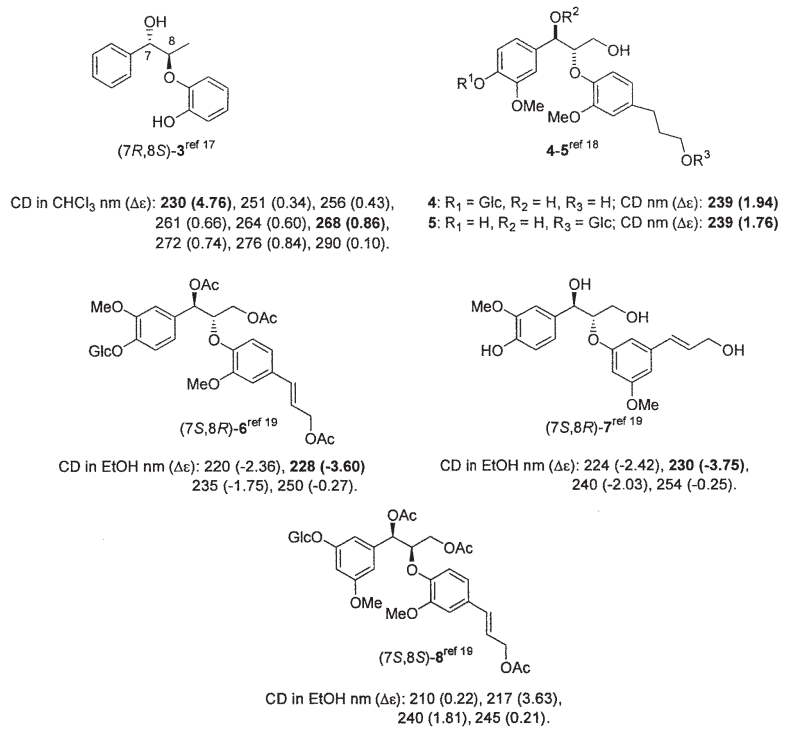

Figure 4. Structures and published CD data of neolignans 4–8 and the related compound 3.

Although the studied erythro-8.O.4'-neolignans (**1a-h**) showed homogeneity in the sense that it was always the 7*S*,8*R*-enantiomers that eluted first and the LC–CD spectra of the first eluted enantiomers showed great similarity or could be correlated with each other, this did not hold for the studied threo-8.O.4'-neolignans (**2b**-**2e**, **2g**, and **2h**; CD data in Table III). Figure 7 shows the LC–CD spectra of the first eluted enantiomers of the measured threo-8.O.4'-neolignans containing allyl side-chain on the ring B (**2b**-**2e**). The CD spectra of **2c** was nearly a mirror image of that of **2b** (Figure 7 and Table III), which implied that the elution order of the enantiomers was inverted in **2c** because of the different substitution pattern of ring A. Furthermore, the CD data also showed great sensitivity to the slight differences in the substitution pattern of the aromatic rings. For instance, the compounds **2b** and **2e** differ only in

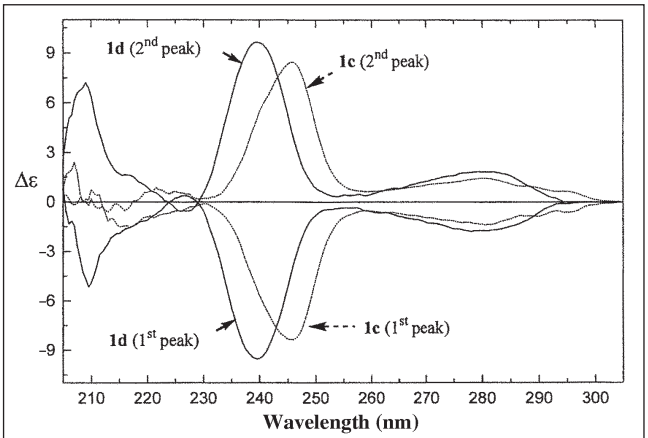

Figure 5. LC–CD spectra of the first and second eluted enantiomers of **1d** (continuous lines) and **1c** (dotted lines).

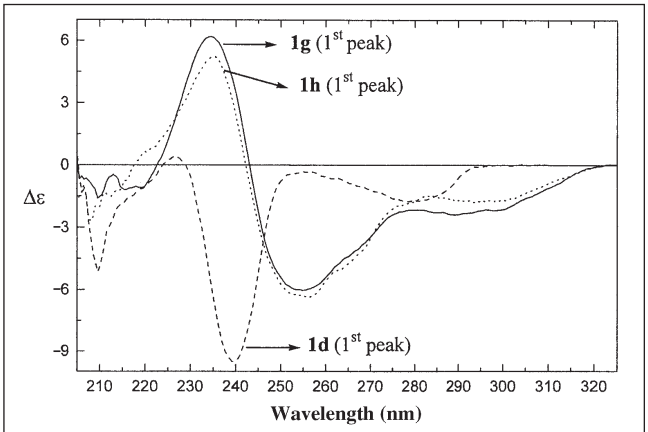

Figure 6. LC–CD spectra of the erythro-8.O.4'-neolignans **1g** (continuous line) and **1h** (dotted line) compared with that of **1d** (broken line).

Table III. CD Data of Threo-8.O.4'-Neolignans (2b-e and 2g-h) Obtained by LC–CD Measurement

Compound	CD data in hexane–isopropanol 9:1 [nm (Δε)]		
2b	275 (0.37), 270 (0.35), 263 (–0.38)	243 (–3.88)	211 (–16.76)
2c	292 (0.40)sh, 287 (0.50)	244 (3.17)	216 (6.90)
2d	279 (–0.86)sh, 276 (–0.94), 267) (–0.65	233 (–10.50)	207 (8.19)
2e	280 (0.59)	235 (–7.04) 230 (–5.89)sh	213 (5.26)
2g	298 (–2.12), 290 (–2.01), 278 (–0.51)	250 (–6.08)	216 (2.74)
2h	297 (–0.87), 291 (–0.84), 275 (0.52)	251 (–2.33)	215 (2.43

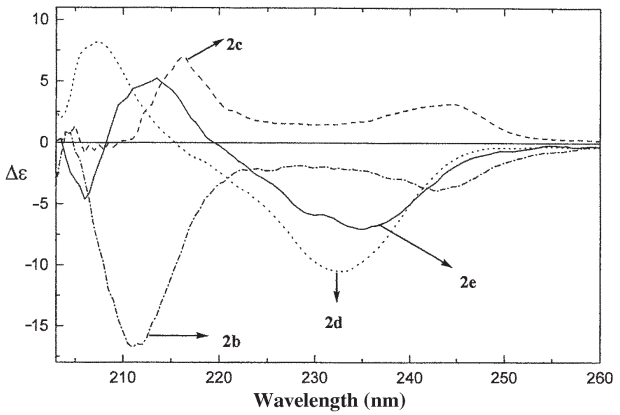

Figure 7. LC–CD spectra of the first eluting enantiomers of the threo-8.O.4'-neolignans for **2b** (----) , **2c** (-----), **2d** (·····), and **2e** (—).

a methoxy group, but their CD spectra were quite different, especially regarding the high-energy transitions [**2b**: 243 (–3.88) and 211 (–16.76); **2e**: 235 (–7.04) and 213 (5.26)]. It seems that the aromatic substitution had a stronger influence on the conformation of the compounds in the threo-series than that of the compounds in the erythro-series, which is reflected in both the reversed elution order and the different CD behavior. This conformational diversity makes their configurational assignment ambiguous, although it is noteworthy that all of the first eluted isomers of the threo-derivatives except **2c** have a negative Cotton effect in the range of 240–260 nm. Greca et al. (19) used CD spectroscopy to determine the configuration of the threo-8.O.4'-neolignan **8** (Figure 4), which has a structure similar to that of **2h** (Figure 1), without offering an explanation. Provided that there is no significant interaction between the two aryl moieties, the Cotton effects derive from two chirally perturbed, substituted benzene chromophore. According to Greca's assignment, it is the aryloxy moiety that determines the signs of the CD bands; namely, if the configuration of C-8 is inverted, the characteristic CD bands change signs. However, this assumption was not verified, and it seems more probable that the benzylic stereogenic center, directly connected to the chromophore, is determinant if there is no significant interaction between the aryl moieties.

Conclusion

The separation of enantiomers of 8.O.4'-type neolignans were achieved in both their erythro- and threo-series (**1a**-**1d**, **1f**-**1h** and **2b**-**2e**, **2g**, and **2h**, respectively) using a Chiralcel OD column. The highest resolution factor was observed in the case of **2d** (R_s = 6.28), yet the neolignans **1e**, **2a**, and **2f** could not be separated at all. Although the efficiency of the separation depends on the substitution pattern of the aryl moieties, this technique can be applied to the optical resolution of synthetic or natural racemates of 8.O.4'-type neolignans to obtain the corresponding optical isomers for studies of structural-activity relationships. The online LC–CD analysis allowed the establishment of a correlation between the absolute configuration of the separated erythro-enantiomers and their characteristic CD transitions. According to this, the intense negative CD transition around 240 nm and the negative transitions around 280 nm derive from the 7*S*,8*R* absolute configuration of erythro-8.O.4'-neolignans. The study of different substituted erythro-enantiomers proved that neither the elution order nor the signs of the characteristic CD bands were affected by the different substitution pattern. These results allow the configurational assignment of previously isolated erythro-8.O.4'-neolignans, for which the CD data were reported and several former assignments were revised. Although the absolute configurations of threo-isomers could not be determined unambiguously from the LC–CD analysis, it was proved that the elution order was reversed for compound **2c** because of the different substitution pattern. Furthermore, the conformation and, therefore, CD transitions of the threo-isomers were found to be more sensitive to the aromatic substitution pattern than those of the erythro-isomers.

Acknowledgments

This article is dedicated to Professor K. Lempert on his 80th birthday.

The authors thank the National Science Foundation (OTKA T-034250, F-043536) for financial support. Tibor Kurtan is indebted to the Hungarian Academy of Sciences for the Bolyai Postdoctoral Fellowship.

References

1. H. Badano and S. Zacchino. Enantioselective synthesis and absolute configuration assignment of erythro-(3,4,5-trimethoxy-7-hydroxy-1'-allyl-2',6'-dimethoxy)-8.O.4'-neolignan, isolated from Mace (*Myristica fragrans*). *J. Nat. Prod.* **51(6):** 1261–65 (1988).
2. S. Zacchino and H. Badano. Enantioselective synthesis and absolute configuration assignment of erythro-(3,4-methylenedioxy-7-hydroxy-1'-allyl-3',5'-dimethoxy)-8.O.4'-neolignans its acetate, isolated from nutmeg (*Myristica fragrans*). *J. Nat. Prod.* **54(1):** 155–60 (1991).

3. J.E. Forrest, R.A. Heacock, and T.P. Forrest. Diarylpropanoids from Nutmeg and Mace (Myristica fragrans Houtt.). *J. Chem. Soc. Perkin Trans. I.* **2:** 205–209 (1974).
4. S. Hada, M. Hattori, Y. Tezuka, T. Kikiuchi, and T. Namba. Constituents of mace. Part 3. Neolignans and lignans from the aril of Myristica fragrans. *Phytochemistry* **27:** 563–68 (1988).
5. A. Isogai, S. Murakoshi, A. Suzuki, and S. Tamura. Structures of dimeric phenylpropanoids from Myristica fragrans. *Agric. Biol. Chem.* **37:** 193–94 (1973).
6. L.E.S. Barata, P.M. Baker, O.R. Gottlieb, and E.A. Rúveda. Neolignans of Virola surinamensis. *Phytochemistry* **17:** 783–86 (1978).
7. S. Cavalcante, M.Yoshida, and O. Gottlieb. The chemistry of Brazilian Miristiceae. Part 26. Lignoids from the fruit of three Virola species. *Phytochemistry* **24:** 1051–55 (1985).
8. P. Ferri and L. Barata. Neolignans and phenylpropanoid from Virola pavonis leaves. *Phytochemistry* **31:** 1375–77 (1992).
9. K. Kónya and S. Antus. Egyszerü szintézisút az antioxidáns tulajdonságú 8.O.4'-típusú neolignánok elöállítására. *Magy Kém. Foly.* **108:** 273 (2002).
10. K. Kónya, Zs. Varga, and S. Antus Antioxidant properties of 8.O.4′-neolignans. *Phytomedicine* **8:** 454 (2001).
11. E. Yashina and Y. Okamoto. Chiral discrimination on polysaccharides derivatives. *Bull. Chem. Soc. Jpn.* **68:** 3289 (1995).
12. Y. Okamoto and E. Yashina. Polysaccharides derivatives for chromatographic separation of enantiomers. *Angew. Chem. Int. Ed.* **37:** 1020 (1998).
13. E. Yashima, Ch. Yamamoto, and Y. Okamoto. Polysaccharide-based chiral LC columns. *Synlett.* **344:** 344–60 (1998).
14. E. Yashima. Polysaccharide-based chiral stationer phases for high-performance liquid chromatographic enantioseparation. *J. Chromatogr. A* **906:** 105 (2001).
15. Y. Okamoto and Y. Kaida. Resolution by high-performance liquid chromatography using polysaccharide carbamates and benzoates as chiral stationary phases. *J. Chromatogr. A* **666:** 403–19 (1994).
16. E. Francotte, R.M. Wolf, and D.J. Lohmann. Chromatographic resolution of racemates on chiral stationary phases: I. Influence of the supramolecular structure of cellullose triacetate. *J. Chromatogr. A* **347:** 25–37 (1985).
17. A. Arnoldi and L. Merlini. Asymmetric synthesis of 3-methyl-2-phenyl-1,4-benzodioxanes. Absolute configuration of the neolignans eusiderin and eusiderin C and D. *J. Chem. Soc. Perkin Trans.* **1:** 2555–57 (1985).
18. N. Matsuda and M. Kikuchi. Studies on the constituents of Lonicera species. X. Neolignan glycosies from the leaves of Lonireca gracilipes var. glandulosa maxim. *Chem. Phram. Bull.* **44(9):** 1676–79 (1996).
19. M.D. Greca, A. Molinaro, P. Monaco, and L. Previtera. Neolignans from Arum italicum. *Phytochemistry* **35(3):** 777–79 (1994).
20. H. Achenbach, J. Grosse, X.A. Dominguez, G. Cano, J.V. Star, L.D.C. Brussolo, G. Munoz, F. Salgado, and L. López. Lignans, neolignans and norneolignans from Krameria cystisoides. *Phytochemistry* **26(4):** 1159–66 (1987).
21. A. Yamamoto, S. Nitta, T. Miyase, A. Ueno, and L.-J. Wu. Phenylethanoid and lignan-iridoid complex glycosides from roots of Buddleja davidii. *Phytochemistry* **32(2):** 421–25 (1993).

Manuscript accepted September 16, 2004.